International Journal of Physics and Applications

**E-ISSN:** 2664-7583
**P-ISSN:** 2664-7575
IJOS 2024; 6(2): 126-129

www.physicsjournal.in
Received: 19-08-2024
Accepted: 25-09-2024

**Khalid Abdullah Najim**
Ministry of Education, Iraq

**Corresponding Author:**
**Khalid Abdullah Najim**
Ministry of education -Iraq

# A hydrothermal synthesis of $TiO_2$ nanostructure and study of its structural, morphology and calculate crystalline size using Debye-scherrer equation

**Khalid Abdullah Najim**

**DOI:** https://DOI.org/10.33545/26647575.2024.v6.i2b.110

**Abstract**
Sample of TiO2 nanoparticles were hydrothermally synthesized and characterizing its structural, optical properties and study its morphology. The crystalline structure and grain sizes were studied by X- Ray Diffractometer, while diameters and shapes of crystalline grains were characterized by Field Emission Scanning Electron Microscope (FESEM). FESEM images has a clear measure of synthesized nanostructure dimensions where the diameter of grains about (117.1 ~ 148.3 nm) which having a spherical grains shape. By XRD characterization lattice spacing ($d_{hkl}$) were measured to be about 1.24 - 3. 24 Aº, and have some peaks in special directions h k l = (110), (020), (120), (121), (220) (112). The mean crystalline size D (nm) is calculated by Debye Scherer equation and it has range 30~200 $nm^3$.

**Keywords:** Hydrothermal reactor, nanostructure, crystalline size, Debye- Scherer

## Introduction
$TiO_2$ is widely applicable in various fields such as (Nonlinear optics, spectral selective, coating for solar energy absorption, electrical battery materials, optical receptors, catalysts in chemical reactions, antibacterial materials, optical painting materials, gas sensors, and cosmetics) [1, 2]. Also Titanium dioxide nanoparticles can be used in medicine for burn treatment, dental materials, coating stainless steel materials, textile fabrics, water treatment, sunscreen lotions, and other applications [3].

It is a chemically stable substance that has excellent semiconductor properties and possesses different crystal structures: Anatase, rutile, and brookite are three different types of minerals. [4] The rutile form is more chemically stable than the other structures but when it comes to the Nano-scale range anatase is the most stable formation compared to the other two phases [5]. It is widely recognized that Anatase exhibits superior Solar-Electric Conversion Efficiency (SECE) and photocatalytic properties compared to Rutile due to its unique electronic structure such as a narrower band gap and faster electron mobility [6]. The performance of photo-catalysis is affected by various aspects such as the crystallization process, composition, grain-surface characteristics, crystallinity, morphology, and particle sizes [7]. The photo- activity of the rutile phase makes it suitable for optical-electronics applications because it has a higher refractive index that induces little scattering inside the crystal structure planes [8]. There are several processes available, such as sol-gel, precipitation and hydrothermal procedures that can be used to generate different shapes of oxide or dioxide nano structures [9]. In some cases hydrothermal reaction method is preferred to synthesize the composites due to its high ability to control the morphology and crystallization process by adjusting the conditions of reactions such as (Duration-solvent type- temperature- pressure), various phases and morphological scales can be achieved in a single step using the hydrothermal method, even at low temperatures with use of strong acid [10]. The crystal structure and mean crystallite size could be investigated by x-ray diffraction analysis. Since X-ray wavelength is in the order of atomic distance in crystal lattice, causes the diffraction of X-ray. When X-ray radiates with certain angle to the crystal consisting of parallel plans with d spacing between them. Reflection of X-rays makes constructive interference when the path- length difference of beams equals an integer multiple of the wavelength.

$$2d \sin\theta = n\lambda \quad (1)$$

Where $d$ is the spacing between diffracting planes, $\theta$ is the incident angle, $n$ is any integer and λ is wavelength of the beam. Debye- Scherer formula could be applied to calculate the crystallite size that state:

$$D = \frac{0.9\lambda}{\beta \cos\theta} \quad (2)$$

Where $D$ is the size of the particle, λ is the X-ray wavelength (1.54 Å) and β is full width at half maximum (FWHM in terms of radian), $\theta$ is the angle between incident x-ray beam and scattered [11]. Lattice parameters for tetragonal structure can be calculate from this equation [12].

$$d_{hkl} = \frac{1}{\sqrt{\frac{h^2+k^2}{a^2}+\frac{l^2}{c^2}}} \quad (3)$$

Equations (1), (2) and (3) will be used to study the synthesized structure and to know its properties.

## Materials and Theoretical Methods

In this work we will use hydrothermal reaction method, this method relies on reactions occurring in solutions [13]. Hydrothermal reaction method has many advantages such as its ability to make the synthesis of nano particles throughout a wide temperatures range starting from low temperatures to extreme degrees of temperatures, In additionally the reactor can be operated at either lower or higher pressures depending on the vapor pressures of the main compositions. More ever it allows to produced nanomaterials that remain stable even at elevated temperatures [14]. Nanostructured materials with high vapor pressure can be synthesized using a hydrothermal autoclave that minimizing the loss of raw materials [15]. To control the morphological properties we added a surfactant material to the mixture before the reaction occurs such as (Ethylene Glycol (EG)), where the surfactant is a substance that restricts the growth of particles in specific directions [16]. In order to synthesis $TiO_2$, we had been mixed precursors that undergo a specific reaction to yield pure $TiO_2$ which consist of (2.5cc) of (Titanium Tetra Iso- Propoxide) (TTIP), (25cc) of $HNO_3$ (diluted to 8 M), (0.055cc) of Ethylene glycol (EG). After putting the precursors inside the baker the mixture was then stirred using a magnetic stirrer to obtain a homogeneous mixture and then we introduced the clear and transparent solution into a (100 cc) Teflon reactor and sealed it tightly using both our hands and a wrench, next we transferred the reactor to the oven at a temperature of (180 °C) for (8 hours), after that we allowed the reactor to cool down to room temperature, once cooled we opened the reactor and proceeded to wash and separate the main product by repeatedly centrifuging, after that we wish it with ethanol and re set the temperature at(120 °C) for (6 hours) to drying the composite and producing $TiO_2$ powder.

## Characterization

### X- Ray Characterization

The crystal structure and lattice parameters were characterized at first by using XRD (X-Ray Diffractometer) that have characteristics of Scan Axis type is (Gonio), Start Position 2θ = (20.0400°), End Position 2θ= (79.9900°), Step Size 2θ = (0.0500), Scan Step Time =(1.0000) s, Scan Type: Pre-set time, Goniometer Radius (240mm), Measurement Temperature =(25 °C), Anode Material is Cu, K-Alpha, wave length λ=(1.54060 Å).

### FESEM Characterization

Morphology and diameters of grains nanostructure were examined using Field Emission Electronic Microscopy (FESEM) with an operating voltage of 18 kV, and at different scales to measure particles lengths and shapes.

## Results and Discussion

### X- Ray Analysis

Based on the X-ray diffraction results, calculations and analysis of these results, comparison with the practical outcomes of other prior studies of the same nanoparticles, it was discovered that the significance of X-ray examinations lies in understanding the structure. The crystalline structure of the substance as well as understanding of material phases, the nature of atom arrangements in crystalline levels and their directions [17]. X-ray diffraction pattern of synthesized Nanostructure is shown in Fig. 1 below that have some special peaks as shown on the chart. Table. 1 We can observe that sample have characteristic peaks which are (110) at 2θ = 28º and (020) at 2θ = 38º, (120) at 2θ = 43º, (121) at 2θ = 53º, (220) at 2θ = 56º, and (112) at 2θ = 69º. Lattice parameters calculated according to eq (3) where (a = b = 4.594 Å), (c= 2.959 Å), and depending on JCPDS card which confirmed that the synthesized sample have a tetragonal crystal type and this structure has rutile phase. Lattice spacing $d_{hkl}$ were measured using Bragg's law of diffraction eq (1) it is ranging between (3.24 Å and 1.24 Å) which are shown in the table. 1 below. Full Width Height Maximum (FWHM) values were also calculated and discovered to be between (0.3936 and 0.4428) (rad) these findings are consistent with those of researches [18-19].

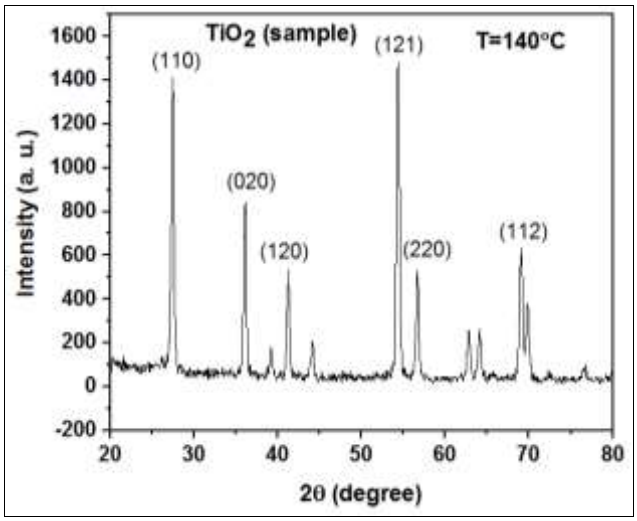


**Fig 1:** XRD pattern by X-ray diffractometer for $TiO_2$

**Table 1:** Shows obtained structural information of $TiO_2$ nanoparticles by XRD-technique

| Peak number | 2θ (Degree) | d (Å) Present Study By X-Ray Difractometer | (HKL) Miller Indices | Intensity (%) | FWHM [2θ] (rad) |
|---|---|---|---|---|---|
| 1 | 27.48˚ | 3.24 | 110 | 95.56 | 0.4428 |
| 2 | 36.19˚ | 2.48 | 011 | 53.49 | 0.3444 |
| 3 | 39.22˚ | 2.29 | 020 | 9.83 | 0.1968 |
| 4 | 41.21˚ | 2.19 | 111 | 29.77 | 0.3444 |
| 5 | 44.15˚ | 2.05 | 120 | 12.11 | 0.2952 |
| 6 | 54.33˚ | 1.68 | 121 | 100 | 0.2460 |
| 7 | 56.70˚ | 1.62 | 220 | 100 | 0.2952 |
| 8 | 62.83˚ | 1.47 | 002 | 1.52 | 0.3936 |
| 9 | 64.12˚ | 1.45 | 130 | 5.25 | 0.3444 |
| 10 | 65.68˚ | 1.42 | 221 | 16.09 | 0.5904 |
| 11 | 69.03˚ | 1.36 | 031 | 1.93 | 0.3936 |
| 12 | 69.79˚ | 1.34 | 112 | 40.06 | 0.1968 |
| 13 | 72.56˚ | 1.30 | 131 | 24.73 | 0.7872 |
| 14 | 76.57˚ | 1.24 | 230 | 1.56 | 0.3936 |

The mean crystallite size calculated by Debye-sheerer formula is shown in table. 2 below

**Table 2:** The mean crystalline size

| 2θ (degree) | d (Å) Present Study By X-Ray Difractometer | FWHM (radian) | D (nm) |
|---|---|---|---|
| 27.48˚ | 3.26 | 0.4428 | 35 |
| 41.21˚ | 2.20 | 0.3444 | 52 |
| 62.83˚ | 1.49 | 0.3936 | 77 |
| 69.79˚ | 1.35 | 0.1968 | 200 |
| 76.57˚ | 1.28 | 0.3936 | 150 |

**FESEM Analysis**

FESEM imaging were taken for different scales as Figure.2 showing below, where the crystalline grains has irregular spherical shape and these particles diameters and lengths has average between (117 to 148 nm), respectively, as determined by the (Picture J software). Because of EG surfactant addition to the reactants the crystal's extremely fast growth and slow nucleation rates encourage the rolling of the titanate layers into three-dimensional structures like Nano grains in small sizes of this grains and that is $TiO_2$ Nano-particles in rutile phase and that study agree with this research [20].

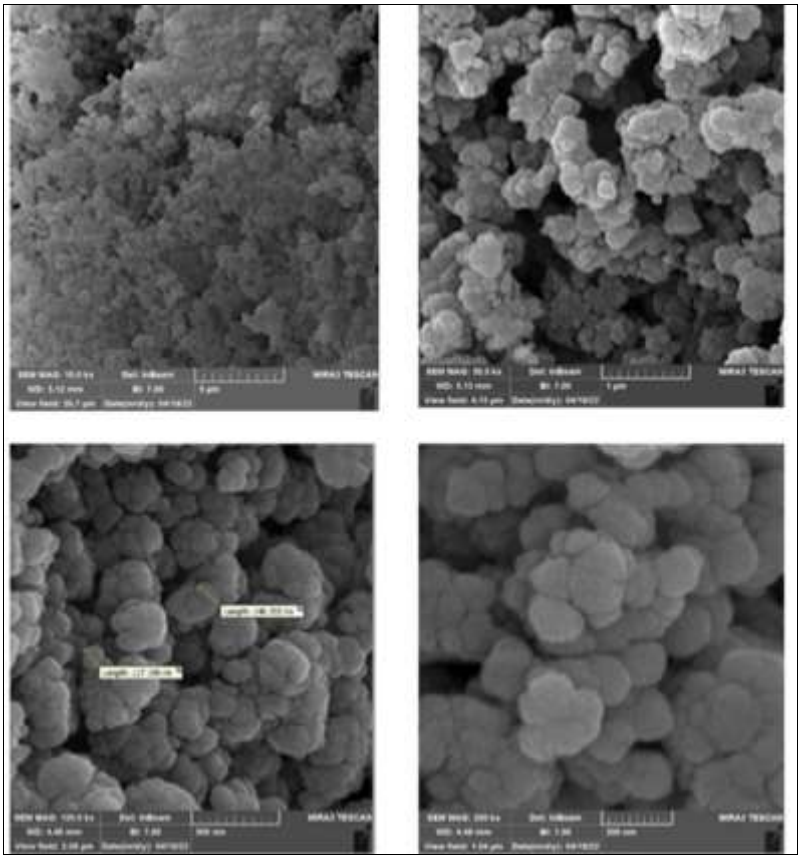

**Fig 2:** FESEM images in different scales: a- (5 µm), b-(1 µm), c-(500 µm), d-(200 µm)

**Conclusions**

According to the characterized and analyzed data for conducted composition, titanium dioxide having a mean particle size ranging from 37 to 200 nm and that size resulting from the addition of the surfactant material ethylene glycol EG, while the length of the particles ranged from 137 to 148 nm. As for the structure it showed structural properties with lattice spacing $d_{hkl}$ ranging from d = (3.24 to 1.24 Aº) as average. Rutile phase structure of $TiO_2$ needs to a higher temperature for a longer duration time more than other types (Anatase and brookite) by comparing with other studies that include preparing of $TiO_2$ in different phases.

**References**


1. Aysin B, Ozturk A, Park J. Silver-loaded $TiO_2$ powders prepared through mechanical ball milling. Ceram Int. 2013;39:7126. Available from: http://dx.doi.org/10.1016/j.ceramint.2013.02.054.
2. Saad AA, Lattieff FA. Nickel and titanium metals for the hydrogen evolution reaction in water electrolysis: A comparative study. Tikrit J Pure Sci. 2023, 28(1). Available from: https://doi.org/10.25130/tjps.v28i1.1267.
3. Twafeeq MT, Mutlak FA-H. Ag/$TiO_2$ core/shell NPs synthesized by laser ablation and its antibacterial activity. Tikrit J Pure Sci. 2021, 26(6). Available from: https://doi.org/10.25130/tjps.
4. Thakur N, Thakur N, Kumar A, *et al*. A critical review on the recent trends of photocatalytic, antibacterial, antioxidant and nanohybrid applications of anatase and rutile $TiO_2$ nanoparticles. Sci Total Environ. 2024;914:169815. Available from: https://doi.org/10.1016/j.scitotenv.2023.169815.
5. Hanaor DAH, Sorrell CC. Review of the anatase to rutile phase transformation. J Mater Sci. 2011;46:855–874. Available from: http://dx.doi.org/10.1007/s10853-010-5113-0.
6. Luttrell T, Halpegamage S, Tao J, Kramer A, Sutter E, Batzill M. Why is anatase a better photocatalyst than rutile? Model studies on epitaxial $TiO_2$ films. Sci Rep. 2014;4:4043. Available from: http://dx.doi.org/10.1038/srep04043.
7. Farooq N, Kallem P, Rehman ZU, *et al*. Recent trends of titania ($TiO_2$) based materials: A review on approaches and potential applications. J King Saud Univ Sci. 2024;36(6):103210. Available from: https://doi.org/10.1016/j.jksus.2024.103210.
8. Ge S, Sang D, Zou L, *et al*. A review on the progress of optoelectronic devices based on $TiO_2$ thin films and nanomaterials. Nanomaterials. 2023;13(7):1141. Available from: https://doi.org/10.3390/nano13071141.
9. Agartan L, Kapusuz D, Park J, Ozturk A. Effect of initial water content and calcination temperature on photocatalytic properties of $TiO_2$ nanopowders synthesized by the sol–gel process. Ceram Int. 2015;41:12788–12797. Available from: http://dx.doi.org/10.1016/j.ceramint.2015.06.114.
10. Ramesh AM, Gangadhar A, Chikkamadaiah M, Shivanna S. Hydrothermal synthesis of $Ga_2O_3/TiO_2$ nanocomposites with highly enhanced solar photocatalysis and their biological interest. J Photochem Photobiol. 2021;6:100020. Available from: https://doi.org/10.1016/j.jpap.2021.100020.
11. Nasiri S, Rabiei M, Palevicius A, *et al*. Modified Scherrer equation to calculate crystal size by XRD with high accuracy, examples $Fe_2O_3$, $TiO_2$ and $V_2O_5$. Nano World J. 2023;3:100015. Available from: https://doi.org/10.1016/j.nwnano.2023.100015.
12. Hassanien AS, Akl AA. Crystal imperfections and Mott parameters of sprayed nanostructure IrO2 thin films. Phys Condens Matter. 2015. Available from: http://dx.doi.org/10.1016/j.physb.2015.05.023.
13. Montazeri-Pour M, Riahi-Noori N, Mehdikhani A. Synthesis of single-phase anatase $TiO_2$ nanoparticles by hydrothermal treatment with application potential for photo anode electrodes of dye-sensitized solar cells. J Ceram Process Res. 2013;14(5):595–600.
14. Gan YX, Jayatissa AH, Yu Z, Chen X, Li M. Hydrothermal synthesis of nanomaterials. J Nanomater. 2020;3:8917013. Available from: https://doi.org/10.1155/2020/8917013.
15. Razooqi MA, Majeed ZN. The effect of copper doping on some structural and electrical properties of titanium dioxide nanofilms. Tikrit J Pure Sci. 2023;28(6):51–57. Available from: https://doi.org/10.25130/tjps.v28i6.1377.
16. Nielsen SO, Srinivas G, Lopez CF, Klein ML. Modeling surfactant adsorption on hydrophobic surfaces. Phys Rev Lett. 2005;94(22):228301. Available from: https://doi.org/10.1103/PhysRevLett.94.228301.
17. Subrahamanyam NA. A Textbook of Optics. 9th ed. Delhi, India; c1977.
18. Vijayalakshmi R, Rajendran V. Synthesis and characterization of nano-$TiO_2$ via different methods. Arch Appl Sci Res. 2012;4(2):1183–1190. Available from: http://scholarsresearchlibrary.com/archive.html.
19. Mosquera E, Herrera-Molina D. Structural and optical properties of $TiO_2$ nanoparticles and their photocatalytic behavior under visible light. Ing Cienc. 2021, 23(2). Available from: https://doi.org/10.25100/iyc.v23i2.10965.
20. Kaur G, Negi P, Kaur M, Sharma R, Konwar RJ, Mahajan A. Morpho-structural and opto-electrical properties of chemically tuned nanostructured $TiO_2$. Ceram Int. 2018;44(15):18484–90. Available from: https://doi.org/10.1016/j.ceramint.2018.07.068.